

Theoretical and Experimental Studies on the Ground- and Excited-State Dipole Moments of 1,4-Naphthoquinone and Its Derivatives

Takehiko Satoh, Mitsutaka Kudoh, Takemasa Tsuji, Shouichi Kita, Toshiaki Mori, and Susumu Sudoh*

Department of Materials Science and Technology, Faculty of Science and Technology, Hirosaki University, Bunkyo-cho, Hirosaki 036-8561

Received November 7, 2006; E-mail: sudoh@cc.hirosaki-u.ac.jp

The dipole moments of the ground- and excited-states of 1,4-naphthoquinone (**1**), 2-chloro-1,4-naphthoquinone (**2**), 2-bromo-1,4-naphthoquinone (**3**), 2-methyl-1,4-naphthoquinone (**4**), 2,3-dichloro-1,4-naphthoquinone (**5**), 2,3-dibromo-1,4-naphthoquinone (**6**), 2-hydroxy-1,4-naphthoquinone (**7**), 3-chloro-2-hydroxy-1,4-naphthoquinone (**8**), 3-bromo-2-hydroxy-1,4-naphthoquinone (**9**), and 2-hydroxy-3-methyl-1,4-naphthoquinone (**10**) were studied from both experimental and theoretical perspectives. For the ground states, the dipole moments of compounds **5**, **8**, and **9** were determined experimentally in dilute solutions (via Debye's method), and compared with those of the other compounds **1**–**4**, **6**, **7**, and **10** which we had already determined. The density functional theory calculations were also performed, revealing a positive correlation with the experimental results. For the excited states, however, the dipole moments of the excited states of compounds **1**–**10** have not yet been studied. In this work, we determined the dipole moments of some of the lower excited states of these compounds using the spectroscopic method. Results revealed the determined excited-state dipole moments exceeded those of the ground state, a finding also supported by the configuration interaction involving one-electron excitations only.

The ground-state dipole moments of the molecule have been determined for many organic and inorganic molecules,[1] since the dipole moment is one of the fundamental physical quantities and provides information concerning the electronic charge distribution in a molecule, of key significance for the molecular structure and reactivity. Moreover, the dipole moment is reflected in the polarity of a molecule and hence plays an important role in molecular interactions between a solute and solvent in a solution.

We had determined the ground-state dipole moments of 1,4-naphthoquinone (**1**) and its derivatives, which were known as some of the various quinones present in the natural products. The compound **1** is a skeleton of Vitamin K_1 and Lapinone, and its hydroxy derivative, 2-hydroxy-1,4-naphthoquinone (**7**), was initially obtained from lawsonia inermis and called lawsone. Compound **7** and its derivatives are known as anticancer and antiviral compounds.[2] Compound **1** can take the following tautomerizations, namely 1,2-naphthoquinone (*ortho*-quinone) and 1,4-naphthoquinone (*para*-quinone), the latter of which is possibly responsible for such activities. In fact there was a report citing tautomerization as one of the requisites for bioactivity.[3] The dipole moment of *para*-quinone is small and 1.21 D for the exact canceling of two carbonyl bond moments,[4] whereas the dipole moment of *ortho*-quinone, conversely, is larger than that of *para*-quinone and 5.72 D for the additive direction of two carbonyl bond moments.[5] This large dipole moment of *ortho*-quinone may have the role of bioactivity. Quinone compounds have also been studied from photochemical perspectives.[6] Recently, Yamaji et al. studied the properties of 1,4-tetracenequinone from photochemical perspectives, and estimated the excited-state dipole moments of 1,4-tetracenequinone as 13.0 D, assuming the ground-state dipole moments, and calculated using a semi-empirical MO method, as 2.6 D.[7] In this case, if the ground-sate dipole moments are known, the excited-state dipole moment can be determined more exactly, so it is important to know the dipole moment of the ground states not in order to understand the molecular interactions with solvent in the solution, but also for estimating the excited-state dipole moments. As well as the ground-state dipole moment, the excited-state dipole moment is vital for observing the interaction between the solvent and solute of the excited state in the solution. Moreover, knowledge of the dipole moment of excited species is useful for the design of non-linear optical materials. There are several methods used to determine the excited-state dipole moment, of which the solvatochromic method was used to determine the excited-state dipole moments of some organic compounds.[8–12] However, for compound **1** and its derivatives, no excited-state dipole moments were determined. The aforementioned quinone compound is a skeleton of an antibiotic, such as adriamycin and daunomycin, so it would be useful to know the excited-state dipole moments for studying the pharmacological mechanism in the local structure.

In this work, we studied the dipole moments of the ground- and excited-states of compound **1** and its derivatives, i.e. 2-chloro-1,4-naphthoquinone (**2**), 2-bromo-1,4-naphthoquinone (**3**), 2-methyl-1,4-naphthoquinone (**4**), 2,3-dichloro-1,4-naphthoquinone (**5**), 2,3-dibromo-1,4-naphthoquinone (**6**), 2-hydroxy-1,4-naphthoquinone (**7**), 3-chloro-2-hydroxy-1,4-naphthoquinone (**8**), 3-bromo-2-hydroxy-1,4-naphthoquinone (**9**), and 2-hydroxy-3-methyl-1,4-naphthoquinone (**10**), from both experimental and theoretical perspectives (Fig. 1).

Published on the web June 13, 2007; doi:10.1246/bcsj.80.1103

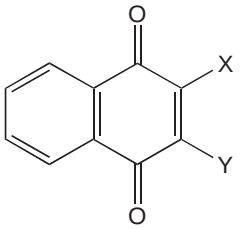

Group I			Group II		
1	X = H	Y = H	**7**	X = OH,	Y = H
2	X = C l,	Y = H	**8**	X = OH,	Y = C l
3	X = B r,	Y = H	**9**	X = OH,	Y = B r
4	X = CH_3,	Y = H	**10**	X = OH,	Y = CH_3
5	X = C l,	Y = C l			
6	X = B r,	Y = B r			

Fig. 1. Molecular skeleton of 1,4-naphthoquinone derivatives.

For the ground state, we had already determined the dipole moments of compounds **1**–**4**, **6**, **7**, and **10** by measuring the dielectric constants and densities of the several dilute benzene solutions,[13] meaning that the ground-state dipole moments of the remaining molecules, i.e. compounds **5**, **8**, and **9**, were determined in this work.

For the excited states, as described above, spectroscopic studies of compounds **1** and its derivatives were performed,[14] although the dipole moments of compounds **1**–**10** have yet to be studied. We tried to determine the excited-state dipole moments of these compounds for the first time using the spectroscopic method.

Experimental and Calculations

Materials. 1,4-Naphthoquinone (**1**) and 2-methyl-1,4-naphthoquinone (**4**) were purchased from Tokyo Kasei Kogyo Co., 2-hydroxy-1,4-naphthoquinone (**7**) and 2,3-dichloro-1,4-naphthoquinone (**5**) were purchased from Kanto Chemical Co. 2-Chloro-1,4-naphthoquinone (**2**) was synthesized via synthesis involving the compound **5**.[15] 2-Hydroxy-3-methyl-1,4-naphthoquinone (**10**) and 3-chloro-2-hydroxy-1,4-naphthoquinone (**8**) were synthesized in accordance with literature.[16,17] 3-Bromo-2-hydroxy-1,4-naphthoquinone (**9**) was synthesized via the same method used to synthesize 2-hydroxy-3-iodo-1,4-naphthoquinone,[18] and 2-bromo-1,4-naphthoquinone (**3**) were synthesized in accordance with the literature.[18] ^{13}C NMR and ^{1}H NMR spectra were used to identify the compounds and those used in the measurement were recrystallized from suitable solvents and checked for purity by TLC.

Determination of the Dipole Moments. Ground State: The ground-state dipole moments were determined by measuring the dielectric constant and density of several dilute solutions of the compounds. The dielectric constant of the dilute solutions was measured at $25 \pm 0.1\,^{\circ}$C using home-made apparatus (via the high frequency bridge method). The densities of the dilute solutions were also measured at $25 \pm 0.1\,^{\circ}$C using an Ostwald-type pycnometer. Benzene, which was carefully purified, was used as a solvent. The concentrations of the solutes ranged from about 0.8×10^{-3} to 4.1×10^{-3} weight fraction. The dipole moments of the molecules were determined from the following equation in Debye units at temperature T:

$$\mu = 0.01281[(P_{2\infty} - R_{MD})T]^{1/2}, \tag{1}$$

in which $P_{2\infty}$ and R_{MD} represent the total polarization of the solute at infinite dilution and the molecular refraction, respectively. The molecular refraction R_{MD} suffers from the contribution of bond refraction and atomic polarization, although that of the atomic polarization is relatively small and difficult to estimate precisely. In this work, the R_{MD} are evaluated from the sum of the bond refractions. We determined the total polarization of the solute at infinite dilution using the Halverstadt and Kumler method and based on the following equation:[19]

$$P_{2\infty} = \frac{3\alpha v_1 M_2}{(\varepsilon_1 + 2)^2} + M_2(v_1 + \beta)\frac{(\varepsilon_1 - 1)}{(\varepsilon_1 + 2)}, \tag{2}$$

in which M_2 is the molecular weight of the solute and ε_1 and v_1 are respectively the dielectric constant and specific volume of the benzene solvent. Dielectric constants and specific volumes were observed for the solvent, and for dilute solutions with variable solute weight fractions. The measured values of the dielectric constants, ε_{12}, and the specific volumes, v_{12}, of the solutions exhibit a linear dependence on the weight fraction, ω_2, of the solute, as given by the equations:

$$\varepsilon_{12} = \varepsilon_1 + \alpha\omega_2, \tag{3}$$

$$v_{12} = v_1 + \beta\omega_2, \tag{4}$$

in which the coefficients α and β are obtained via the least-square fitting of the above equations. The total polarizations of the solute at infinite dilution, $P_{2\infty}$, were calculated by the Eq. 2 using coefficients α and β in Eqs. 3 and 4.

Excited State: Certain methods are used to determine the excited-state dipole moments, i.e. electric dichroism,[20] fluorescence polarization,[21] the Stark splitting of rotational levels,[22–24] microwave conductivity,[25] thermochromic shift,[26] and solvatochromic shift. Of these, the most popular is currently the solvatochromic method used to determine excited-state dipole moments.[8–12]

In order to obtain the dipole moment of excited states within an equilibrium molecular structure, we usually have to use the Stokes shifts.[27] We found, however, that compound **1** and its derivatives emit phosphorescence only in the solution,[28] so we were unable to determine the excited-state dipole moments of the equilibrium molecular structure. Therefore, we estimated the dipole moment of the Frank–Condon excited-state using the McRae equation and based on the shift of UV–vis spectra in various solvents. The McRae equation used to determine the excited-state dipole moment was given as:[29]

$$\Delta\tilde{\nu} = K\frac{n^2 - 1}{2n^2 + 1} + L\left(\frac{\varepsilon - 1}{\varepsilon + 2} - \frac{n^2 - 1}{n^2 + 2}\right) + M\left(\frac{\varepsilon - 1}{\varepsilon + 2} - \frac{n^2 - 1}{n^2 + 2}\right)^2, \tag{5}$$

where $\Delta\tilde{\nu}$ is the shift of absorption maxima (hexane is chosen as a reference solvent) and ε and n are respectively the dielectric constant and refractive index of the solvents. The first term with K represents two types of interaction, one between the induced dipoles of the solute and solvent, and the other between the dipole of the solute and the induced dipole of the solvent respectively. The second term, meanwhile, with L represents the interaction between the dipoles of the solute and solvent, while the final term with M represents the interaction between the dipole of the solvent and the induced dipole of the solute. Robertson et al. showed that

Table 1. Weight Fractions (ω_2), Dielectric Constants (ε_{12}) and Specific Volumes (v_{12}) of Compounds **5**, **8**, and **9**

Compound	$\omega_2/10^{-3}$	ε_{12}	$v_{12}/\mathrm{cm^3\,g^{-1}}$
5	0.8201	2.2782	1.14421
	1.1646	2.2809	1.14411
	1.5721	2.2837	1.14392
	1.9480	2.2857	1.14378
	2.5664	2.2900	1.14344
8	0.7063	2.2793	1.14427
	1.1056	2.2834	1.14411
	1.4692	2.2877	1.14396
	1.8530	2.2902	1.14381
	2.3443	2.2950	1.14358
9	1.0548	2.2812	1.14407
	1.7576	2.2878	1.14375
	2.4523	2.2943	1.14348
	3.1819	2.2998	1.14323
	4.1215	2.3075	1.14278

the last term was small and could be neglected.[30] For the non-polar solvent, the second and final terms are zero, and the constant K of the first term can be estimated from the slope of the plot of $\Delta\tilde{\nu}$ vs $[(n^2-1)/(2n^2+1)]$. Here, we assumed the first term to be \constant and considered the second term only. The excited-state dipole moments were determined from the constant L of the second term, which was obtained as a slope of a plot of $\Delta\tilde{\nu}$ vs $[(\varepsilon-1)/(\varepsilon+2)-(n^2-1)/(n^2+2)]$. The constant L was expressed as the following equation:

$$L=\frac{2}{hca_0{}^3}(\mu^{\mathrm{g}}-\mu^{\mathrm{e}})\mu^{\mathrm{g}}, \tag{6}$$

Here, μ^{g} and μ^{e} are the ground- and excited-state dipole moments, respectively, and a_0 indicates the Onsager cavity radii, while the constants h and c are the Plank constant and light velocity.

UV–Vis Spectra. The solvents used in the measurement were chosen from those which were found to be sufficient to measure the higher excited states, and they were then purified by distillation. The UV–vis absorption spectra were measured on a HITACHI U-3500 spectrophotometer at room temperature.

Calculations. The ground-state dipole moments were calculated using the program package Gaussian 98.[31] Three types of methods, i.e. Hartree–Fock self consistent field method (HF), Moller–Plesset second-order perturbation theory (MP2), and Becke, Lee, Yang, and Parr functional (B3LYP) method, were used for the calculations and the basis set 6-311G** was employed for all calculations. Calculations of the excited-state dipole moments were performed using the same program package as the ground state. The configuration interaction method with one-electron excitations only (CIS) was employed and the basis sets 6-31+G** was used. The molecular structures used for the CIS calculations were those of the ground state, which were optimized by B3LYP/6-311G** level calculations. The calculations were performed at the Research Center for Computational Science (Okazaki, Japan) and the Information Center of Hirosaki University.

Results and Discussion

Dipole Moments of the Ground State. Experimental Results: The ground-state dipole moments of the compounds **5**, **8**, and **9** were measured at 25 °C in benzene solutions. In Table 1, we showed the weight fractions, ω_2, dielectric constants, ε_{12}, and specific volumes, v_{12}, of compounds **5**, **8**, and **9**. The total polarization, $P_{2\infty}$, of the solute and molar refraction, R_{MD}, for the sodium D line were shown in Table 2 along with the values, α, β, ε_1, and v_1 in Eqs. 2 and 3 which were obtained by the least-square fitting of linear relations, as given in Fig. 2. The ground-state dipole moments, which were calculated from Eq. 1 using $P_{2\infty}$ given in Table 2, were also presented in the same table (see Table 5 for the ground-state dipole moments of other compounds). The dipole moments of the derivatives of compound **1** exceeded those of compound **1** except for compound **4**. In this compound, the directions of the dipole moments of compound **1** and the methyl group were seemingly opposite. Since the dipole moment is a vector, the dipole moments of many organic compounds have been reasonably explained based on the bond or group moment.[32] For mono-substituted benzene derivatives, the group moments of –OH, Cl, Br, and $-CH_3$ were reported as 1.28, 1.59, 1.57, and 0.37 D, respectively. For the derivatives of compound **1**, we obtained group moments of 1.60, 1.04, 1.02, and 0.27 D for –OH, Cl, Br, and $-CH_3$, respectively (see Scheme 1). There were some differences in the group moments of –OH, Cl, Br, and $-CH_3$ at the derivatives of benzene and compound **1**, which may be attributable to the carbonyl group. For the group moments of Cl and Br, we found that the considerable differences could be partially attributed to the calculated atomic charge on both atoms. The atomic charges on the Cl and

Table 2. Dipole Moments and Other Quantities Used for the Determination of Dipole Moments of Compounds **5**, **8**, and **9**

	5	**8**	**9**
ε_1	2.2730	2.2729	2.2727
α	6.635	9.482	8.530
$v_1/\mathrm{g^{-1}\,cm^3}$	1.14461	1.14457	1.14450
$\beta/\mathrm{g^{-1}\,cm^3}$	−0.442	−0.418	−0.411
$M/\mathrm{g\,mol^{-1}}$	227.046	208.60	253.051
$R_{\mathrm{MD}}/\mathrm{cm^3}$	52.116	48.806	51.686
$P_{2\infty}/\mathrm{cm^3}$	330.839	417.14	461.263
μ^{g}/D	3.69	4.25	4.48

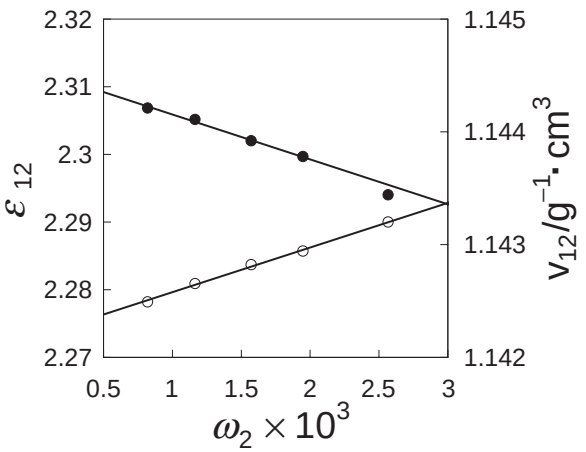

Fig. 2. Dielectric constant (●) and specific volume (○) vs weight fractions of compound **5**.

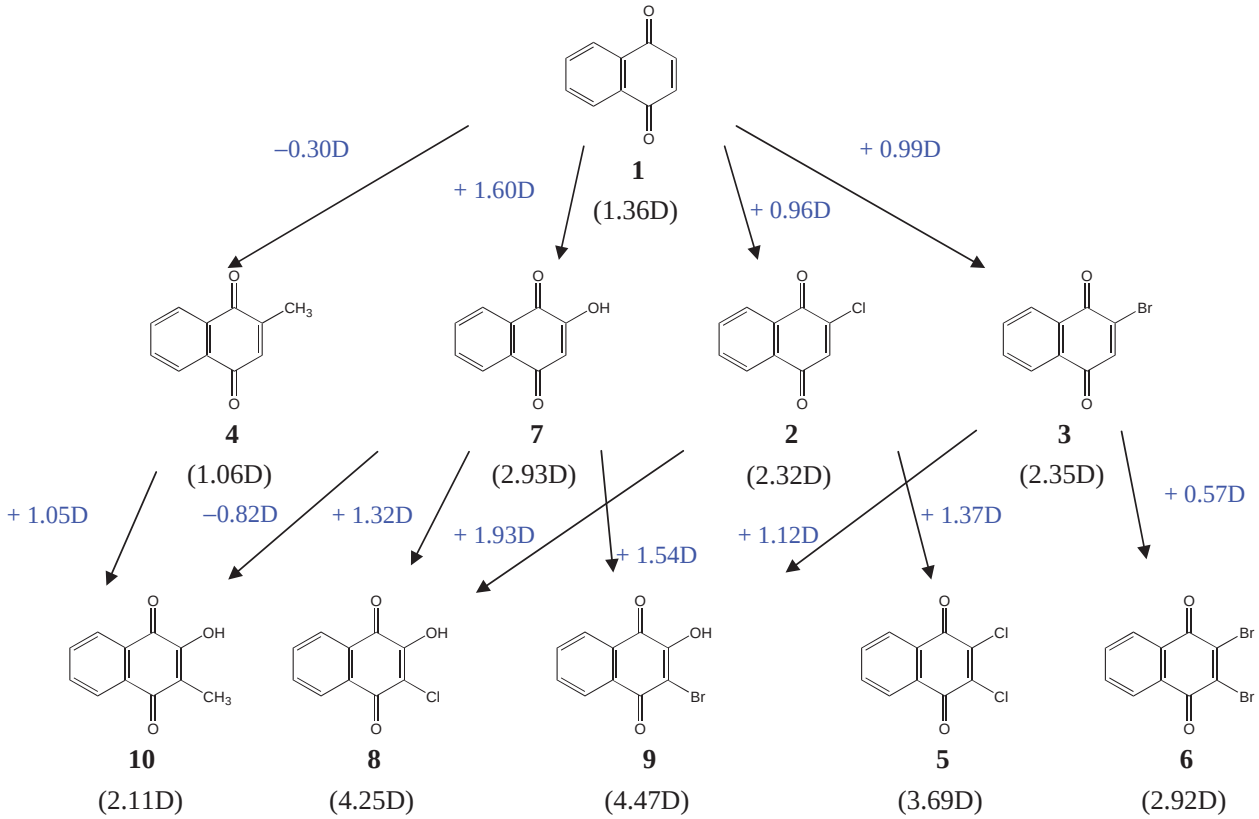

Scheme 1.

Table 3. Bond Lengths of Compounds **1**–**10** (/Å)[a)]

Compound	r_1	r_2	r_3	r_4	r_5	r_6	r_7	r_8	r_9	r_{10}	r_{11}	r_{12}	r_{13}
1	1.1892	1.1892	1.4888	1.4888	1.3216	1.4943	1.4943	1.3921	1.3866	1.3866	1.3822	1.3822	1.3875
2	1.2115	1.2182	1.5032	1.4816	1.3402	1.4929	1.4906	1.4041	1.3967	1.3953	1.3907	1.3908	1.3963
3	1.2117	1.2181	1.5021	1.4839	1.3401	1.4945	1.4899	1.4039	1.3968	1.3954	1.3907	1.3907	1.3964
4	1.2193	1.2203	1.4992	1.4781	1.3454	1.4915	1.4919	1.4038	1.3967	1.3954	1.3905	1.3907	1.3968
5	1.2115	1.2115	1.5036	1.5036	1.3501	1.4887	1.4887	1.4015	1.3962	1.3962	1.3906	1.3906	1.3961
6	1.2117	1.2116	1.5058	1.5058	1.3499	1.4894	1.4894	1.4006	1.3966	1.3966	1.3903	1.3903	1.3963
7	1.2235	1.2212	1.5002	1.4642	1.3492	1.4731	1.5048	1.4058	1.3975	1.3926	1.3902	1.3902	1.3961
8	1.2234	1.2147	1.4964	1.4800	1.3542	1.4717	1.5032	1.4043	1.3965	1.3928	1.3906	1.3931	1.3955
9	1.2234	1.2148	1.4986	1.4794	1.354	1.4711	1.5247	1.4040	1.3967	1.393	1.3905	1.3931	1.3955
10	1.2234	1.2148	1.4986	1.4794	1.354	1.4711	1.5047	1.4040	1.3967	1.393	1.3906	1.3931	1.3955

a) See Scheme 2.

Br atoms of chlorobenzene and bromobenzene by B3LYP/6-311G** level were −0.074 and −0.030, respectively, but 0.011 and 0.056 for compounds **2** and **3** (as q_{H13} in Table 4) and the bond moments were consequently inverse in direction, with greatly reduced contribution to total moment. The substituent effect estimated from di-substituted compounds, however, gave reasonable values for the –OH, –Cl groups, i.e. for the –OH group the increased values were 1.12 D from compounds **3** to **9** and 1.05 D from compounds **4** to **10**, and for the –Cl group, the values were 1.35 D from compounds **2** to **5** and 1.32 D from compounds **7** to **8**, respectively. This was due to the effect of the carbonyl groups being cancelled. For $–CH_3$ and –Br groups, however, we were unable to observe any effect similar to the –OH, –Cl groups, meaning the former case might be fortuitous.

Results of Calculations. Molecular Structure and Charge Density: The geometrical parameters of the molecule were all optimized at B3LYP/6-311G** and MP2/6-311G** level calculations, while the bond lengths calculated by the B3LYP/6-311G** level were shown in Table 3 (see Scheme 2). Clear cut differences are found in the carbonyl (C=O) bond lengths between groups I (quinone group; without the hydroxy group as a substituent) and II (lawsone group; with the hydroxy group as a substituent). In group II, r_1 is longer than that of group I, due to the existence of hydroxy group in the vicinity. A similar feature is apparent at bond lengths r_6 and r_7. In group II, r_6 was shorter than that of group I, and r_7 longer than that of group I. In particular, r_3 of group II has been significantly affected under the substitution and became longer than that of group II. At the benzenoid

Table 4. Atomic Charge with Hydrogen Atom[a)]

Compound	q_{H1}	q_{H2}	q_{H3}	q_{H4}	q_{H5}	q_{H6}	q_{H7}	q_{H8}	q_9	q_{10}	q_{11}	q_{12}	q_{H13}	q_{H14}
1	0.2436	0.0458	0.0458	0.2436	0.0902	0.0358	0.0358	0.0902	−0.1313	−0.1313	−0.284	−0.284	—	—
2	0.3583	−0.2674	0.1714	0.2483	0.0953	0.0404	0.0399	0.096	−0.1249	−0.1279	−0.2588	−0.282	0.0114	—
3	0.3164	−0.2214	0.1267	0.247	0.0954	0.0399	0.0400	0.0957	−0.1276	−0.1278	−0.2585	−0.2816	0.0557	—
4	0.2526	−0.1353	0.0525	0.2474	0.0876	0.0349	0.0337	0.0892	−0.1135	−0.1317	−0.2858	−0.2905	0.1588	—
5	0.3711	−0.1804	−0.1804	0.3712	0.1001	0.0433	0.0433	0.1001	−0.1212	−0.1213	−0.2585	−0.2584	0.0456	0.0456
6	0.3292	−0.1803	−0.1803	0.3292	0.0999	0.0425	0.0425	0.0999	−0.1233	−0.1233	−0.2586	−0.2586	0.0907	0.0907
7	0.2207	0.1698	0.0218	0.2524	0.0894	0.0432	0.0329	0.1001	−0.1193	−0.1337	−0.3225	−0.2988	−0.056	—
8	0.2398	0.2971	−0.3229	0.3693	0.0951	0.0468	0.0374	0.1043	−0.1168	−0.1268	−0.3221	−0.2724	−0.0388	0.0195
9	0.2374	0.2423	−0.2779	0.3271	0.0945	0.0467	0.0371	0.1047	−0.1169	−0.1288	−0.3223	−0.2717	−0.0364	0.0641
10	0.2443	0.184	−0.1758	0.2586	0.0881	0.0409	0.0321	0.0968	−0.1214	−0.1137	−0.3291	−0.2959	−0.0735	0.1647

a) See Scheme 2.

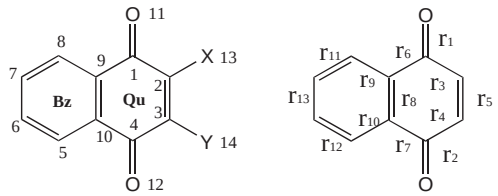

Scheme 2.

ring (B_z), however, there was little difference among the compounds. For the 2- and 2,3-substituted derivatives, the benzenoid ring has no substitution effect, despite the fact that significant changes were found in the quinonoid ring (Q_u). The HOMO of compound **1** has less contribution from a quinonoid moiety (see the HOMO at a footnote in Table 14), so we could see that there was little influence in the benzenoid ring from the substitution of 2- or/ 3-positions from the first-order perturbation theory.

The atomic charges calculated at B3LYP/6-311G** level are given in Table 4 (see Scheme 2). The negative charge was mainly located at the oxygen atom of the carbonyl groups. As we found that there was the difference of the bond length between two groups I and II, the atomic charge on oxygen showed characteristic differences between the two groups. The values of q_{11} and q_{12} were virtually equal for the compounds of group I, whereas those of q_{11} and q_{12} of the group II compounds differed significantly and q_{11}, which was the carbonyl oxygen neighboring the hydroxy group, was more negative than q_{12}. This tendency corresponded to the fact that r_2 of group II was longer than that of group I, in other words, the double bond character was reduced for an ionic structure ($-C{=}O \leftrightarrow -C^{+}-O^{-}$). A charge separation from benzenoid to quinonoid rings was also observed. This charge separation had a positive correlation with the ground-state dipole moments of compounds **1**–**10** described below.

Dipole Moments of the Ground State: We performed ab initio molecular orbital calculations using the HF method, using various basis sets for the compounds **1**–**10**.[13] For these compounds, the calculated ground-state dipole moments by the HF method, using the basis set 6-311G**, conformed to the experimental ground-state dipole moments. This work also involved more sophisticated calculations, such as the application of the density functional theory and perturbation method for example. For the calculation, the B3LYP/6-311G** and MP2/6-311G** levels were used. The calculated results are shown in Table 5 along with the experimental ground-state dipole moments. In Fig. 3, we showed the correlation between calculated and the experimental dipole moments, with the best correlation occurring between the results of the B3LYP/6-311G** level calculation and the experimental results. The dipole moment has been well explained from a qualitative perspective, based on the bond or group moments. Here, we tried to explain the ground-state dipole moments of compounds **1**–**10**, based on the intramolecular charge transfer. The atomic charge may be partitioned into two rings (see Scheme 2) and the charges partitioned were given in Table 6. Figure 4 showed the correlation between the calculated dipole moment and the partial charge of the ring (B_z). We obtained a positive correlation. However, regarding the contribution of the intramolecular charge transfer to the dipole moment, although not precisely distinguished from the bond moment of the substitute, the intramolecular charge transfer might nevertheless be recognized to some extent in compounds **1**–**10**. In compound **4**, we see that the electronic property of the methyl group clearly differs from that of the halogen groups, i.e. the C–H bond moment of the $-CH_3$ group contributes to the total dipole moment in the reverse direction.

For compound **7** and its halogeno-derivatives, there may be two conformers (types I and II, in which an intramolecular

Table 5. Dipole Moments of 1,4-Naphthoquinone and Its Derivatives (/D)

Compound	Exptl.[a)]	Calc.		
		HF[b)]	B3LYP[c)]	MP2[d)]
1	1.33	1.35	1.36	1.43
2	2.32	3.00	2.76	2.95
3	2.35	2.86	2.58	2.81
4	1.06	1.09	1.04	1.18
5	3.69[e)]	4.00	3.58	3.90
6	2.92	3.59	3.13	3.49
7	2.93	3.22	2.99	3.47
8	4.25[e)]	4.93	4.38	5.06
9	4.47[e)]	4.77	4.16	4.90
10	2.11	2.61	2.30	2.86

a) Ref. 13. b) HF/6-311G**//HF/6-311G**. c) B3LYP/6-311G**//B3LYP/6-311G**. d) MP2/6-311G**//MP2/6-311G**. e) This work.

hydrogen bond may occur) as shown in Scheme 3. We previously suggested the possibility of equilibrium between two types of conformers, namely I and II, for compounds **7–9** from the IR spectra in CCl_4.[33] The dipole moments and total energies of the two conformers, as calculated by the B3LYP/6-311G** level, were shown in Tables 7 and 8, respectively. We calculated the dipole moment and the total energy of the conformer, in which the O–H bond is vertical to the molecular plane (type III (see Scheme 3)), and the results were also given in Tables 7 and 8, respectively. The differences of the total energy among three types were shown in Table 7 where ΔE_1 and ΔE_2 are the differences between types I and III, and types I and II, respectively. Although not fully optimized, the molecular structure of type III was found to be in a transition state, which was verified by the vibration calculation of type III. The value of ΔE_1 was considered to be the internal rotation barrier of the OH bond. Based on Tables 7 and 8, we can see that the calculated total energy of type I was lowest among the three types for all compounds **7–10**, and the dipole moments of type I also correlated well to the experimental values for all compounds **7–10**. In addition, the values of ΔE_1 are similar among the four compounds **7–10** and relatively low, but it seems difficult for the OH bond to rotate from type I to type II and overcome this potential barrier at room temperature. Moreover, based on the value of ΔE_2 we found the population of type II to be small compared with type I, assuming the presence of an equilibrium. Our calculated results revealed that type I was a main conformer at compounds **7–10**. The fact that the experimental dipole moments were smaller than the calculated dipole moments of type I and that the calculated dipole moment of type II was smaller than that of type I, however,

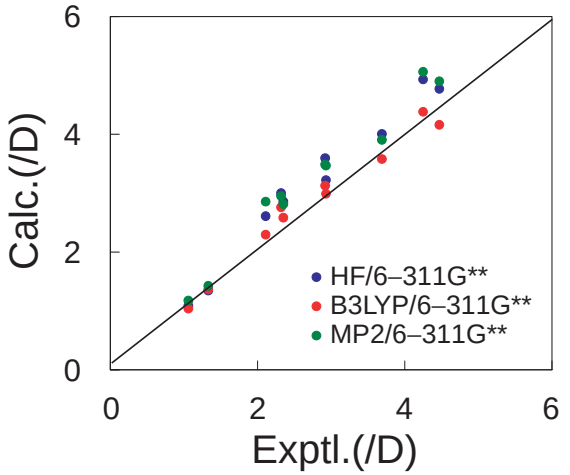

Fig. 3. The correlation of the ground-state dipole moment between the calculated μ^g_{calc} and experimental μ^g_{exptl} values.

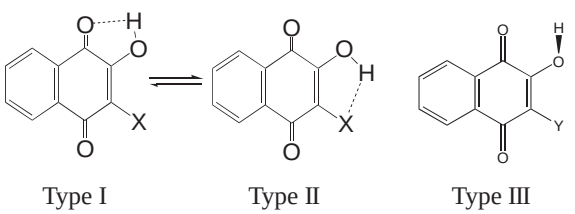

Scheme 3.

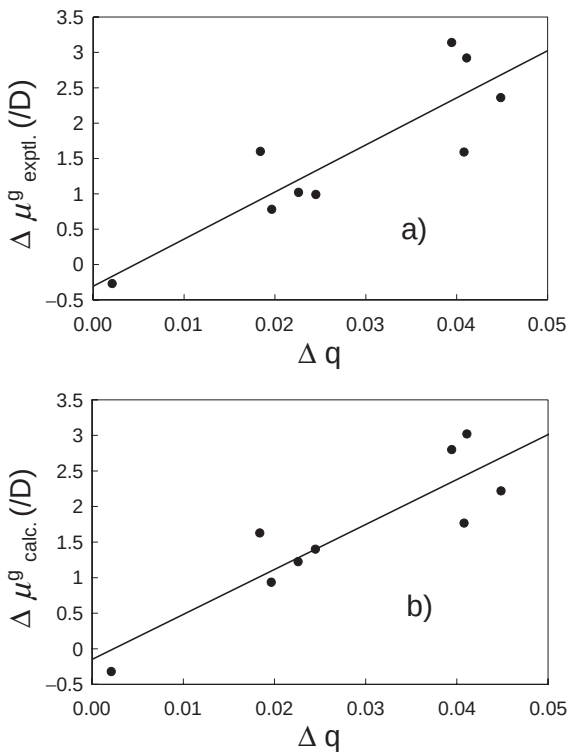

Fig. 4. The relation between $\Delta\mu^g$ and Δq. a) $\Delta\mu^g_{exptl}$ vs Δq, b) $\Delta\mu^g_{calc}$ vs Δq.

Table 6. Charge Partitions and Dipole Moments Differences from 1,4-Naphthoquinone (/D)[a)]

Compound	q_{B_z}	q_{Qu}	Δq	$\mu^g_{exptl.}$	$\Delta\mu^g_{exptl.}$	$\mu^g_{calc.}$ [b)]	$\Delta\mu^g_{calc.}$
1	0.1207	−0.1207	0.000	1.33	0.00	1.36	0.00
2	0.1452	−0.1452	0.0245	2.32	0.99	2.76	1.40
3	0.1433	−0.1433	0.0226	2.35	1.02	2.58	1.22
4	0.1228	−0.1228	0.0021	1.06	−0.27	1.04	−0.32
5	0.1656	−0.1656	0.0449	3.69	2.36	3.58	2.22
6	0.1615	−0.1615	0.0408	2.92	1.59	3.13	1.77
7	0.1391	−0.1391	0.0184	2.93	1.6	2.99	1.63
8	0.1618	−0.1618	0.0411	4.25	2.92	4.38	3.02
9	0.1602	−0.1602	0.0395	4.47	3.14	4.16	2.80
10	0.1404	−0.1404	0.0197	2.11	0.78	2.30	0.94

a) $q_{B_z} = [q_{H5} + q_{H6} + q_{H7} + q_{H8}] + (q_9 + q_{10})/2$, $\Delta q(\mathbf{i}) = q_{B_z}(\mathbf{i}) - q_{B_z}(\mathbf{1})\Delta\mu^g_{explt.}(\mathbf{i}) = \mu^g_{explt.}(\mathbf{i}) - \mu^g_{explt.}(\mathbf{1})$, $\Delta\mu^g_{calc}(\mathbf{i}) = \mu^g_{calc}(\mathbf{i}) - \mu^g_{calc}(\mathbf{1})$. b) B3LYP/6-311G** calculations.

supports our previous hypothesis from the IR spectra, namely that the type II conformer might be found in CCl_4.[33]

Dipole Moments of the Excited-State. Experimental Results: The UV–vis spectra of compound **1** and its derivatives studied in this work essentially showed similar characteristics due to their similar molecular framework. For example, the UV–vis spectra of compounds **1**, **7**, and **9** in hexane were shown in Fig. 5. The absorption spectra of compound **1** revealed two peaks at around 335 and 245 nm, in the former of which a shoulder at shorter wavelength was found. At the mono-substituted derivatives of compounds **1** and **7**, the absorption at 245 nm of compound **1** splits into four absorption peaks at 239, 246, 270, and 279 nm respectively. On the other hand, at the di-substituted derivative of compounds **1** and **9**, the absorption band at 335 nm of compound **1** splits into two absorption bands at 332 and 385 nm. We found that the absorption bands of compounds **1**–**10** were divided to two regions, one of which was the band at 335 nm, which was composed of two bands, and the second of which the band at 245 nm, which was overlapped by four absorption bands, respectively. These characteristics of the absorption spectra of compounds **1**–**10** were supported by our CIS calculations. Figure 6 showed the spectral peaks of the CIS calculations alongside the observed spectrum, revealing good correlation between the observed and calculated spectral patterns. We henceforth showed the absorption bands examined in Fig. 7, and termed them A to F in order from longer to shorter wavelength. The absorption maxima of compounds **1**–**10** in hexane were given in Table 9. Furthermore absorption bands B, D, and F were assigned to the charge-transfer band from benzenoid to quinonoid, and bands A, C, and E assigned to the quinonoid or benzenoid band based on the CIS calculations (see Table 14). These characteristics of the UV–vis spectra of the quinones match the classification by Singh et al.[14a] Umadevi et al. had assigned bands corresponding to the A and B absorptions of compound **4** to n–π^* transitions,[14b] but we assigned these bands as π–π^* transitions, based on the fact that n–π^* transition is forbidden and has less intensity, if any, and the dipole moments of these excited-states, moreover, exceeded those of the ground states (described below), and provided these transitions were subject to the n–π^* transitions, the excited-states should have small dipole

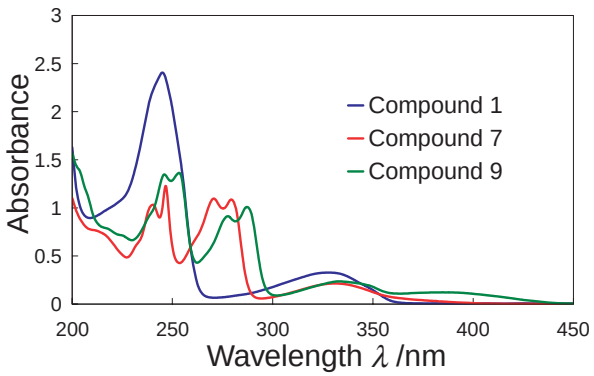

Fig. 5. UV–vis spectra of 1,4-naphthoquinone (**1**), 2-hydroxy-1,4-naphthoquinone (**7**), and 3-bromo-2-hydroxy-1,4-naphthoquinone (**9**).

Table 7. Ground-State Dipole Moments of Compounds **7**–**10** (/D)

Compound	Exptl.[a)]	Type I	Type II	Type III
7	2.93	2.99	0.40	2.19
8	4.25	4.38	1.92	3.30
9	4.47	4.16	1.79	3.11
10	2.11	2.3	0.90	1.88

a) From Table 5.

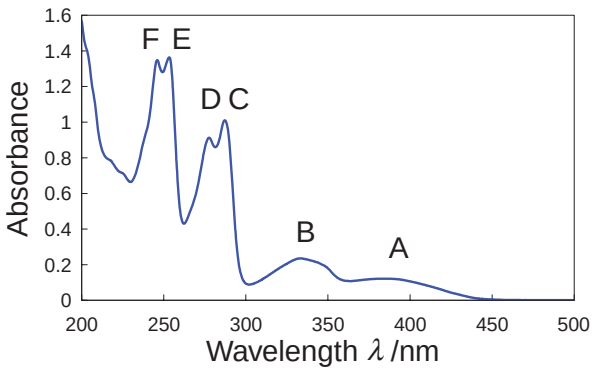

Fig. 6. UV–vis spectrum of 3-bromo-2-hydroxy-1,4-naphthoquinone (**9**) in hexane.

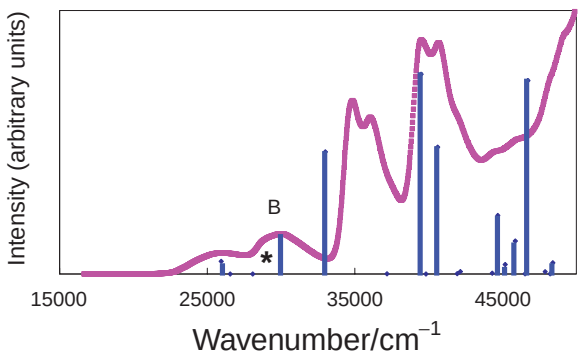

Fig. 7. Calculated spectral peaks and observed spectra of compound **1** in hexane. The calculated spectral peaks were shifted to match the peak signed as * to the band B.

Table 8. Total Energy and Differences of Total Energies between Two Conformers (/au)

Compound	E(type I)	E(type II)	E(type III)	ΔE_1[a)]	ΔE_2[b)]
7	−610.5061	−610.4948	−610.4825	0.0236	0.0113
8	−1070.1225	−1070.1156	−1070.0997	0.0228	0.0070
9	−3184.0442	−3184.0379	−3184.0206	0.0236	0.0063
10	−649.8376	−649.8243	−649.8148	0.0228	0.0133

a) $\Delta E_1 = E$(type III) − E(type I). b) $\Delta E_2 = E$(type II) − E(type I).

Table 9. Absorption Maxima of 1,4-Naphthoquinone and Its Derivatives in Hexane ($/10^4\,cm^{-1}$)

	1		**2**		**3**		**4**		**5**		**6**		**7**		**8**		**9**		**10**	
	exptl.	calc.	exptl.	calc.	exptl.	calc.	exptl.	calc.	exptl.	calc.	exptl.	calc.	exptl.	calc.	exptl.	calc.	exptl.	calc.	exptl.	calc.
1(n–π^*)[a]	—	3.465	—	3.524	—	3.498	—	3.489	—	3.592	—	3.547	—	3.646	—	3.929	—	3.704	—	3.937
2(n–π^*)[a]	—	3.628	—	3.677	—	3.677	—	3.670	—	3.725	—	3.717	—	3.897	—	3.632	—	3.917	—	3.628
A	2.861	4.053	2.814	3.966	2.927	3.947	2.887	3.994	2.791	3.880	2.773	3.846	2.701	3.751	2.658	3.710	2.599	3.619	2.714	3.650
B	3.049	4.246	2.987	4.214	3.251	4.211	3.038	4.258	3.001	4.193	2.974	4.188	3.019	4.207	3.003	4.182	3.008	4.178	3.047	4.220
C	3.925	5.478	3.696	5.470	3.497	5.460	3.794	5.493	3.584	5.463	3.504	5.442	3.577	5.534	3.524	5.518	3.453	5.507	3.529	5.522
D	4.006	5.640	3.820	5.610	3.626	5.588	3.943	5.659	3.704	5.598	3.626	5.569	3.693	5.687	3.636	5.675	3.600	5.663	3.696	5.692
E	4.090	6.521	3.971	6.463	3.965	6.557	4.019	6.527	3.971	6.453	3.953	6.331	4.052	6.483	3.971	6.390	3.928	6.396	3.928	6.343
F	4.172	6.609	4.065	6.587	4.209	6.610	4.116	6.664	4.065	6.579	4.052	6.528	4.149	6.605	4.085	6.524	4.072	6.516	4.132	6.548

a) We could not decide precisely in this work, so the calculated values were given only.

moments compared with those of the ground state. In Table 9 we also showed the wavelength calculated using the CIS method. The absorption maxima expect three maxima (the band F of compound **3** and the band E of both compounds **9** and **10**) to be shifted to a longer wavelength as the solvent polarity increases. The wavenumber at the absorption maxima and the shifts ($\Delta\tilde{\nu}$) from that in hexane were shown in Table 10. The correlation between $\Delta\tilde{\nu}$ and McRae solvent parameters $[(\varepsilon-1)/(\varepsilon+2)-(n^2-1)/(n^2+2)]$ (see Table 11) were shown in Fig. 8, which also showed the case of absorption band E of compound **7** as an example. Based on the least-square fitting of the relation between $\Delta\tilde{\nu}$ and $[(\varepsilon-1)/(\varepsilon+2)-(n^2-1)/(n^2+2)]$, we obtained the slopes, i.e. the constant L in the McRae equation, with the results given in Table 12. The excited-states dipole moments were determined using the slope L and the Onsager cavity radii, which were obtained from the molecular structures optimized by the B3LYP/6-311G** level and subsequently shown in Table 13. The resulting experimental excited-state dipole moments were shown in Table 13 where the ground-state dipole moments and the results of CIS calculations (described below) were also given for comparison. Virtually all the dipole moments of six excited-states exceeded those of the ground-state dipole moments, except for compounds **3** (the excited state of the band F), **9** and **10** (both the excited states of the band E). It was reasonable that the excited-states dipole moments corresponding to bands B, D, and F exceeded those of the ground state, since these bands were assigned to intramolecular charge-transfer bands. For compounds **1** and **4**, there were very significant experimental dipole moments of some excited states, which would also be obtainable via intramolecular charge transfer. It is interesting to note that the μ^{e}_{exptl} of the band F at compound **3** has a negative sign, which suggests that the dipole direction of this excited state is opposite to that of the ground-state dipole moment. The direction of the calculated corresponding excited-state dipole moment, however, was the same as that of the ground-state dipole and did not correlate to the experimental result. For the higher excited states, the CIS calculations must be refined.

Results of the CIS Calculations: The theoretical calculations of the excited-state dipole moments of **1**–**10** were performed using the CIS method, and the basis set 6-31+G** was applied to all compounds, while the molecular structures used for the CIS calculations were optimized by B3LYP/6-311G** level. In Table 13, we showed the theoretical excited-state dipole moments alongside the experimental results. The calculated excited-state dipole moments exceeded those of the ground-state without exception, but were smaller than those of the experimental dipole moments of the excited states. We found that comparatively strong correlation between the experimental and calculation results for compounds with large ground-state dipole moments, but this was much weaker for compounds in which the ground-state dipole moments were small, as for compounds **1** and **4**. In particular, some excited-states of compound **4** revealed an abnormally large dipole moment compared with calculations. If the positive and negative charges are separated by 4 Å in a molecule, the dipole moment would become about 19.2 D, meaning the excited states of band D would have a virtually ionic structure within

Table 10. Shifts of the Absorption Maxima from Those in Hexane ($\Delta\nu/10^2\,cm^{-1}$)

	C_6H_{14}	Cycl-C_6H_{12}	C_7H_{16}	CH_3Cl	THF	CH_2Cl_2	CH_2ClCH_2Cl
1	0	−8.720	−0.5250	—	−1.731	−11.01	—
2	0	−1.976	—	—	—	−2.631	—
3	×[a)]	0	—	—	15.81	1.422	—
4	0	—	−0.3467	−4.380	—	−5.013	—
5	0	−0.3302	−0.2300	−0.2300	—	−4.747	−4.751
6	0	−10.72	—	—	—	−12.99	—
7	0	−1.007	2.072	−0.6735	−3.740	−4.747	−4.751
8	0	−1.993	—	—	—	—	−2.653
9	0	—	−0.9923	−2.308	—	−2.308	−2.308
10	0	—	−0.6819	—	—	−1.022	—

a) This compound was not soluble in hexane.

Table 11. McRae Solvent Parameter

Solvent	Dielectric constant ε	Refractive index n	Parameter
C_6H_{14}	1.880	1.3723	−0.0006
Cycl-C_6H_{12}	2.024	1.4235	−0.0004
C_7H_{16}	1.841	1.3547	0.0012
C_5H_{12}	1.857	1.3580	0.0026
CCl_2CCl_2	2.28	1.5032	0.0034
Benzene	2.274	1.4979	0.005
CCl_4	2.229	1.4574	0.0181
Toluene	2.381	1.4941	0.024
CH_3Cl	4.806	1.4429	0.2941
THF	7.58	1.4050	0.4418
CH_2Cl_2	8.93	1.4212	0.4719
CH_2ClCH_2Cl	10.37	1.4421	0.4928

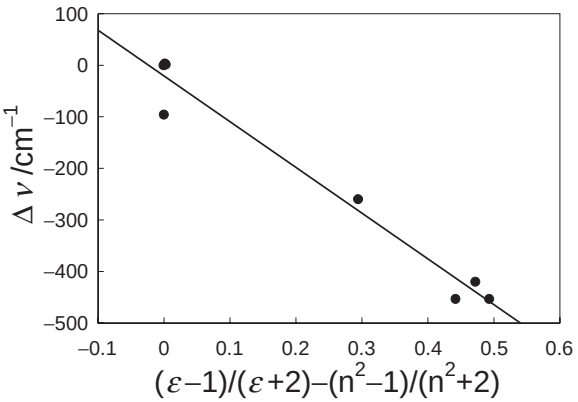

Fig. 8. The relation between the shift of absorption maxima $\Delta\nu$ and McRae parameter.

Table 12. The Slope ($cm^{-1}/10^3$) of the Relation between $\Delta\nu$ and McRae Solvent Parameter Obtained by Least-Square Method for Absorption Bands of A to F

Compound	A	B	C	D	E	F
1	b)	−0.8600	−0.9987	−0.7571	−1.248	−1.347
2	b)	−1.292	−0.8859	−1.583	−0.5303	−0.4173
3	−2.214	−1.621	a)	a)	−1.272	1.723
4	b)	−1.131	−0.6517	−1.916	−1.092	−1.025
5	b)	−0.5478	−1.214	−0.6009	−0.6188	−0.7641
6	−1.286	−1.591	−0.7680	−1.039	−1.608	−1.617
7	b)	−0.7022	−1.342	−0.9916	−0.8866	−0.9425
8	−0.5513	−1.364	−0.7154	−0.2344	−0.1593	−0.3359
9	−0.2303	−1.729	−0.9768	−1.131	0.2825	−0.1691
10	−1.716	−1.572	−0.7313	−0.6025	0.3322	−0.1448

a) For compound **3**, we estimated the slopes for the excited states corresponding to the bands A, B, E, and F. b) The slopes of absorption band A for compounds **1**, **2**, **4**, **5**, and **7** were not decided (see Table 9).

a molecule. Since the value of μ^e_{exptl} was obtained from the term of the dipole–dipole interaction between the solute and solvent, for compounds **1** and **4**, featuring only slight ground-state dipole moments, the solvent effect might be small enough to still ensure sufficient accuracy. The CIS results, however, were accepted reasonably, despite some problems involving certain differences in magnitude between the theoretical and experimental results, and in contrast to the experimental results, at the higher excited states of bands E and F of compounds **7**–**10**, the calculated excited-state dipole moments were smaller than those of the ground state. Such behavior was experienced at the lower excited state A of compounds **8**–**10**, so it may be necessary to refine both μ^e_{exptl} and μ^e_{calc} values.

The MO's concerning the electronic transition are useful for the assignment of the absorption bands and the change in the electronic charge of a molecule. In Table 14, we showed the calculated results of the configuration interactions for compound **1** as an example. The highest occupied MO (HOMO), lowest unoccupied MO (LUMO), and certain other MO's were

Table 13. Experimental and Theoretical Dipole Moments of Excited- and Ground-States (/D)

Compound	μ^g	μ^e												Cavity radii
		A		B		C		D		E		F		
		$\mu^e_{exptl.}$	$\mu^e_{clac.}$	$\mu^e_{exptl.}$	$\mu^e_{clac.}$	μ^e_{exptl}	$\mu^e_{clac.}$	$\mu^e_{exptl.}$	$\mu^e_{clac.}$	$\mu^e_{exptl.}$	$\mu^e_{clac.}$	$\mu^e_{exptl.}$	$\mu^e_{clac.}$	a_0/Å
1	1.33	a)	4.15	7.58	4.91	8.59	3.46	6.84	3.87	10.41	3.02	11.12	4.80	4.60
2	2.32	a)	5.03	7.43	6.73	5.82	5.08	8.58	5.67	4.42	4.15	3.97	6.40	4.52
3	2.35	11.41	4.65	8.98	6.77	a)	5.08	a)	5.67	7.55	6.18	−4.70	2.25	4.59
4	1.06	a)	3.02	11.79	4.39	7.24	2.89	19.24	3.37	11.42	2.51	10.79	3.98	4.66
5	3.69	a)	5.14	5.22	7.92	7.08	6.04	5.37	6.77	5.42	4.82	5.83	6.58	4.70
6	2.92	7.73	4.28	8.87	7.82	5.79	5.79	6.81	6.31	8.93	2.90	8.97	6.25	4.79
7	2.93	a)	3.68	5.14	6.52	7.16	4.76	6.06	5.03	5.73	2.28	5.90	1.81	4.53
8	4.25	5.53	4.10	7.42	8.29	5.91	6.13	4.79	6.59	4.62	2.90	5.03	3.00	4.63
9	4.47	4.98	3.59	8.31	8.28	6.64	5.96	6.98	6.48	3.84	3.12	4.85	1.57	4.64
10	2.11	9.33	1.97	8.72	5.95	5.19	3.77	4.64	4.29	0.71	4.35	2.72	1.51	4.47

a) The dipole moments $\mu^e_{exptl.}$ of these excited states could not be estimated (see Tables 9 and 12).

Table 14. The Results of CIS Calculations of Compound **1**[a)]

Excited state	Wavenumber/cm^{-1}	Intensity	$\Psi_{i\to j}$	C_{ij}	$\Psi_{i\to j}$	C_{ij}	$\Psi_{i\to j}$	C_{ij}
1	34651	0	38 → 42	0.6010	37 → 66	−0.1844	37 → 45	0.1698
2	36277	0	37 → 42	0.5885	38 → 66	−0.1906	38 → 45	0.1866
A	40532	0.0127	40 → 42	0.6104	41 → 45	0.2038	39 → 42	0.1928
B	42459	0.1211	41 → 42	0.6192	40 → 45	−0.2390	41 → 48	0.1858
C	54783	0.4907	40 → 45	0.5565	41 → 42	0.2936	41 → 48	−0.2097
D	56395	0.6310	41 → 45	0.4536	40 → 42	−0.2959	39 → 42	0.2929
E	65206	0.6107	40 → 48	0.5248	41 → 45	−0.2980	36 → 42	0.1900
F	66085	0.6822	41 → 48	0.5871	40 → 45	0.2637	40 → 50	−0.1447

a) Some MO's were shown at footnote, and the 41th MO was the highest occupied MO. $\Psi_{i\to j}$ denotes the electron transition from i-th MO to j-th MO, and C_{ij} coefficient of configuration $\Psi_{i\to j}$.

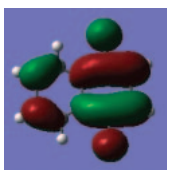
LUMO(42)

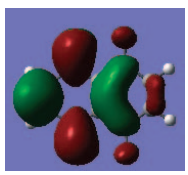
LUMO+3(45)

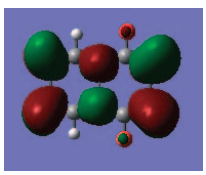
LUMO+6(48)

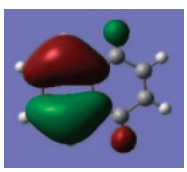
HOMO(41)

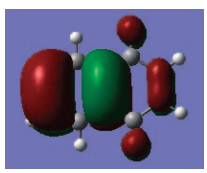
HOMO-1(40)

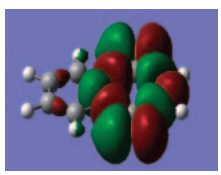
HOMO-3(38)

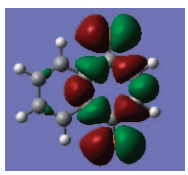
HOMO-4(37)

shown in a footnote to Table 14. From this Table, we could clearly see that the transition from HOMO to LUMO brought out the charge transfer from the benzenoid to the quinonoid with the increase in dipole moment, and that the lowest two transitions in which MO's of LUMO, HOMO−3, and HOMO−4 were concerned were assigned to n–π^* transitions, while absorption bands A to F where MO's related to the transition were all π type MO's, and were assigned to π–π^* transitions. In particular, bands B and C were the charge-transfer band from the benzenoid to the quinonoid ring and the resulting excited-state dipole moments exceeded those of the ground state. Based on the CIS calculations, the lower excited-states of compounds **2**–**10** were also assigned to π–π^* transitions.[34]

Conclusion

The ground-state dipole moments of 2,3-dichloro-1,4-naphthoquinone (**5**), 3-chloro-2-hydroxy-1,4-naphthoquinone (**8**), and 3-bromo-2-hydroxy-1,4-naphthoquinone (**9**) were determined in addition to the other 1,4-naphthoquinone derivatives previously reported, and for compounds **1**–**10**, the excited-state dipole moments were determined from the UV–vis spectra using the McRae equation. The DFT calculations on the ground-state dipole moments and the CIS calculations on the excited-states were also simultaneously performed. The ground-state dipole moments are well explained, based on the B3LYP/6-311G** level calculations, while CIS calculations were used to properly assign the UV–vis spectra of compounds **1**–**10**. The

experimental excited-state dipole moments exceeded those of the ground-state dipole moments for the compounds studied here. The CIS calculations also revealed larger dipole moments during excited states and supported the experimental results. The intramolecular charge transfer provides an adequate explanation for the large excited-state dipole moments.

Supporting Information

UV–vis spectra of Compounds **1**, **2**, **4**, **7**, and **9** studied and the results of CIS calculations of compounds **1**–**10** with graphical MO's are available free of charge on the web at: http://www.csj.jp/journals/bcsj/.

References

1 a) A. L. McClellan, *Tables of Experimental Dipole Moments*, W. H. Freeman and Company, San Francisco and London, **1963**. b) *CRC Handbook of Chemistry and Physics*, 80th ed., ed. by D. R. Lide, CRC Press Boca Raton, New York, Washinton, D.C., **1999**–**2000**, pp. 9–42.

2 a) K. V. Rao, *Cancer Chemother.* **1974**, *4*, 11. b) J. C. da Silveira, *Phytochemistry* **1975**, *14*, 1829.

3 S. da G. M. Portugal, J. O. M. Herrera, I. M. Brinn, *Bull. Chem. Soc. Jpn.* **1997**, *70*, 2071.

4 C. C. Meredith, L. Westland, G. F. Wright, *J. Am. Chem. Soc.* **1957**, *79*, 2385.

5 S. Nagakura, A. Kuboyama, *J. Am. Chem. Soc.* **1954**, *76*, 1003.

6 T. Itoh, *J. Chem. Phys.* **1987**, *87*, 4361.

7 M. Yamaji, K. Takehira, T. Itoh, H. Shizuka, S. Tobita, *Phys. Chem. Chem. Phys.* **2001**, *3*, 5470. Recently, we determined the dipole moments of some of 1,4-*para*-quinones. The dipole moment of 1,4-tetracenequinone was determined as 3.5 D in benzene solution. By using this value, the excited-state dipole moment of 1,4-tetracenequinone will be reduced to somewhat small dipole moment.

8 N. Kitamura, E. Sakuda, *J. Phys. Chem.* **2005**, *109*, 7429.

9 A. Masternak, G. Wenska, J. Milecki, B. Skalski, S. Franzen, *J. Phys. Chem.* **2005**, *109*, 759.

10 M. Ravi, A. Samanta, T. P. Radhakrishnan, *J. Phys. Chem.* **1994**, *98*, 9133.

11 S. Kumar, S. K. Ramesh, R. C. Rastogi, *Spectrochim. Acta, Part A* **2001**, *57*, 291.

12 N. Sharma, S. K. Jain, R. C. Rastogi, *Bull. Chem. Soc. Jpn.* **2003**, *76*, 1741.

13 M. Kudoh, S. Katagiri, S. Sudoh, *Sci. Rep. Hirosaki Univ.* **1997**, *44*, 57.

14 a) I. Singh, R. T. Ogata, R. E. Moor, C. W. J. Chang, P. J. Scheur, *Tetrahedron* **1968**, *24*, 6053. b) M. Umadevi, A. Ramasubbu, P. Vanelle, V. Ramakrishnan, *J. Raman Spectrosc.* **2003**, *34*, 112.

15 P. V. Bedworth, J. W. Perry, S. R. Marder, *Chem. Commun.* **1997**, 1353.

16 F. Radt, *Elsevier's Encycl. Org. Compd.* **1952**, *12B*, 3069.

17 F. Radt, *Elsevier's Encycl. Org. Compd.* **1952**, *12B*, 3119.

18 F. Kehrmann, B. Mascioni, *Ber.* **1895**, *27*, 345.

19 I. F. Halverstadt, W. D. Kumler, *J. Am. Chem. Soc.* **1942**, *64*, 2988.

20 J. Czekalla, *Z. Elektrochem.* **1960**, *64*, 1221.

21 J. Czekalla, *Chimia* **1961**, *15*, 26.

22 J. R. Lombardi, *J. Am. Chem. Soc.* **1970**, *92*, 1831.

23 T. M. Korter, D. R. Borst, C. J. Butler, D. W. Pratt, *J. Am. Chem. Soc.* **2001**, *123*, 96.

24 J. A. Reese, T. V. Nguyen, T. M. Korter, D. W. Pratt, *J. Am. Chem. Soc.* **2004**, *126*, 11387.

25 M. P. Hass, J. M. Warman, *Chem. Phys.* **1982**, *73*, 35.

26 E. Z. Lippert, *Z. Naturforsch., A: Phys. Sci.* **1955**, *10*, 541.

27 Y. Ooshika, *J. Phys. Chem.* **1954**, *9*, 594. The dipole moments of the excited-state at equilibrium structure were obtained from the Storks shift (the difference between 0–0 transitions of the absorption and fluorescence spectra).

28 For compounds **1** and **4**, Itoh reported that compound **1** and **4** in the vapor-phase emit weak E-type delayed fluorescence as well as phosphorescence.[6] Umadevi et al., however, obtained the results that compound **4** in the solution emits fluorescence only,[14b] so we were unable to determine the excited-state dipole moments of the equilibrium molecular structure at the excited-state by using the spectroscopic method.

29 E. G. McRae, *J. Phys. Chem.* **1957**, *61*, 562.

30 W. W. Robertson, A. D. King, Jr., O. E. Weigang, Jr., *J. Chem. Phys.* **1961**, *35*, 464.

31 M. J. Frisch, G. W. Trucks, H. B. Schlegel, G. E. Scuseria, A. D. Daniels, K. N. Kudin, M. C. Strain, O. Farkas, J. Tomasi, V. Barone, M. Cossi, R. Cammi, B. Mennucci, C. Pomelli, C. Adamo, S. Clifford, J. Ochterski, G. A. Petersson, P. Y. Ayala, Q. Cui, K. Morokuma, P. Salvador, J. J. Dannenberg, D. K. Malick, A. D. Rabuck, K. Raghavachari, J. B. Foresman, J. Cioslowski, J. V. Ortiz, A. G. Baboul, B. B. Stefanov, G. Liu, A. Liashenko, P. Piskorz, I. Komaromi, R. Gomperts, R. L. Martin, D. J. Fox, T. Keith, M. A. Al-Laham, C. Y. Peng, A. Nanayakkara, M. Challacombe, P. M. W. Gill, B. Johnson, W. Chen, M. W. Wong, J. L. Andres, C. Gonzalez, M. Head-Gordon, E. S. Replogle, J. A. Pople, *Gaussian 98 (Revision A.11)*, Gaussian, Inc., Pittsburgh PA, **2001**.

32 V. I. Minkin, O. A. Osipov, Y. A. Zhdanov, *Dipole Moments in Organic Chemistry*, Plenum Press, New York, London, **1970**, Chap. III, p. 86.

33 T. Satoh, M. Kudoh, T. Tsuji, H. Mastuda, S. Sudoh, in press.

34 The CIS calculation results of compounds **1**–**10** were available from the Supporting Information.